Article

Effect of Samples Length on the Characteristics of Moisture Transfer and Shrinkage of *Eucalyptus urophylla* Wood during Conventional Drying

Honghai Liu [1,2,*], **Mengqing Ke [1]**, **Ting Zhou [1]** and **Xinlu Sun [1]**

[1] College of Furnishings and Industrial Design, Nanjing Forestry University, Nanjing 210037, China; kmq@njfu.edu.cn (M.K.); muyit@njfu.edu.cn (T.Z.); sunxinlu1@njfu.edu.cn (X.S.)

[2] Jiangsu Co-Innovation Center of Efficient Processing and Utilization of Forest Resources, Nanjing Forestry University, Nanjing 210037, China

* Correspondence: liuhonghai2020@njfu.edu.cn

Abstract: Moisture transfer influences wood deformation and moisture content (MC) distribution during conventional drying of *Eucalyptus urophylla* wood. This study aims to investigate the effect of sample length (30, 100, and 200 mm) on moisture distribution and transfer in different directions and locations and on deformation of wood. The results showed that when the MC was above the fiber saturated point (FSP), the drying rate decreases exponentially with an increase of sample length; however, below the FSP, there was no obvious relationship between the drying rate and sample length and above the FSP, the moisture distribution was non-uniform along tangential, radial, and longitudinal directions and became even below the FSP, which was more significant in the middle location of wood. The greatest MC differences occurred between the surface and sub-central layers along the tangential and radial direction, which were between the end and sub-middle locations along the longitudinal direction. The effect of sample length on the MC distribution and MC differences along wood in the three directions depended on locations and the MC stage of wood; most of the free water and bound water transferred from the wood central to the ends along the longitudinal direction for three sets of samples. Bound water diffusion significantly slowed as the sample length exceeded 200 mm; sample length affects wood collapse and its recovery, but the drying rate has a lesser effect on collapse for samples with a length below 200 mm.

Keywords: *Eucalyptus urophylla*; dimension; moisture; transfer; collapse; conventional drying

1. Introduction

Trees within the Eucalyptus genus are widely planted in certain countries to meet the demands from the wood industry and environmental protection due to their good biological features responding to fertilization, resistance to pests, and strong adaptations to the environment [1–4]. Most Eucalyptus wood are commonly used to produce low-value wood composite boards, pulp, and bio-refineries, etc., because they have certain technical difficulties related to processing, such as high internal stress and drying problems of internal checking, collapse, and a high transverse shrinkage [5–7]. However, the use of Eucalyptus wood as a resource of lumber for higher quality wood products has recently received extensive interest in some countries [8–10].

High-quality drying of Eucalyptus wood is the most critical problem for their higher value-added products [11]. As known, wood is composed mainly of cellulose, hemicellulose, and lignin. Hemicellulose, which contains a high number of hydroxyl groups, is responsible for the wood's hygroscopicity and moisture content (MC) [12]. The performance of wood materials and products is strongly associated to their MC [13–17], which significantly affects wood properties, processing, and use [18–20]. Therefore, drying is needed to decrease wood MC to an appropriate level to meet the requirements of wooden

products. There are several drying methods used in the wood industry, in which the conventional kiln drying has dominated in the drying of lumbers due to its low cost and wide adaptability [21,22]. Although it is difficult to dry the refractory Eucalyptus wood owing to their natural propensity to internal checking and collapse, some Eucalyptus wood have been dried successfully at the commercial level using conventional kiln drying [23]. The studies showed that relatively thin wood (<20 mm) can be dried with less internal checking and collapse if they are pre-treated by air drying from green to the fiber saturated point (FSP). Furthermore, other reasonable pre-treatments, such as pre-steaming [24], pre-boiling [25], and pre-freezing [26], are all effective to lessen the prevalence of collapse and checking and to promote drying of Eucalyptus wood.

Collapse, defined as a deform that occurs above the FSP, is considered to be caused by the capillary tensions development during the early stage of drying. The explanation assumes that the major cause for collapse is that the cell wall cannot withstand the surface tension of free water being removed from the cell lumens [27]. The free water in wood is removed by capillary forces, whereas the bound water removal is driven by diffusion due to the MC gradient [28,29]. Diffusion of water in wood is affected by anatomical structure, MC, and diffusion direction. The moisture transfer in wood in the longitudinal direction is the highest, followed by the radial direction, and is the lowest in the tangential direction [30–33]. For hardwood species, anatomical structure such as vessels, rays, and pits also influence the movement of water [34,35].

Hence, a good understanding of the relationship between collapse and moisture removal in wood is needed to successfully dry these species into commercial solid wood products. However, most studies have focused on the relationship between MC and the physical, mechanical, and chemical properties of wood after drying [36–38]. Studies evaluating the transport of water in wood from different directions and its effect on collapse are rare. The purpose of this study is to investigate the effect of sample length on moisture transfer in wood in the tangential, radial, and longitudinal directions and the collapse of *Eucalyptus urophylla × E. grandis*.

2. Materials and Methods

2.1. Materials

Three fast-growing *Eucalyptus urophylla × E. grandis* trees (6 years old) were purchased in Guangxi Provence, China. After being felled, one tree was processed into 4 logs with a length of 1000 mm, taken from a height of 300 mm from the root. The logs were wrapped with plastic film and then were transported to Nanjing Forestry University; thereafter, they were processed into lumbers of 30 × 30 × 1000 mm (tangential × radial × longitudinal) using a band saw and a single blade saw. Finally, four lumbers prepared from one log were selected and sawn into three sets of end-matched and defect-free samples. The lengths of the samples were 30, 100, and 150 mm, respectively (Figure 1). Two slices were cut in both ends of a lumber using a circle saw and used for the determination of the MC of the lumber. The mass of each slice was measured using an electronic balance and then they were dried at 103 °C in an oven for 24 h to obtain the oven-dry mass (zero MC). The MC of the slices was determined based on the oven-dry mass. The initial MC of the samples used in this study was approximately 100%.

2.2. Equipment and Devices

The drying equipment includes a constant temperature and humidity chamber (DF-408, Nanjing Defu test equipment Co., Ltd., Nanjing, China); an electric heating oven (DHG-905-386-III, Shanghai Cimo medical equipment manufacturing Co., Ltd., Shanghai, China); a digital vernier caliper (CD-20CPX, Japan Mitutoyo Co., Ltd, Tokyo, Japan, 0.01 mm); and an electronic balance (JA5003N, Shanghai precision scientific instrument Co., Ltd., Shanghai, China, 0.001 g).
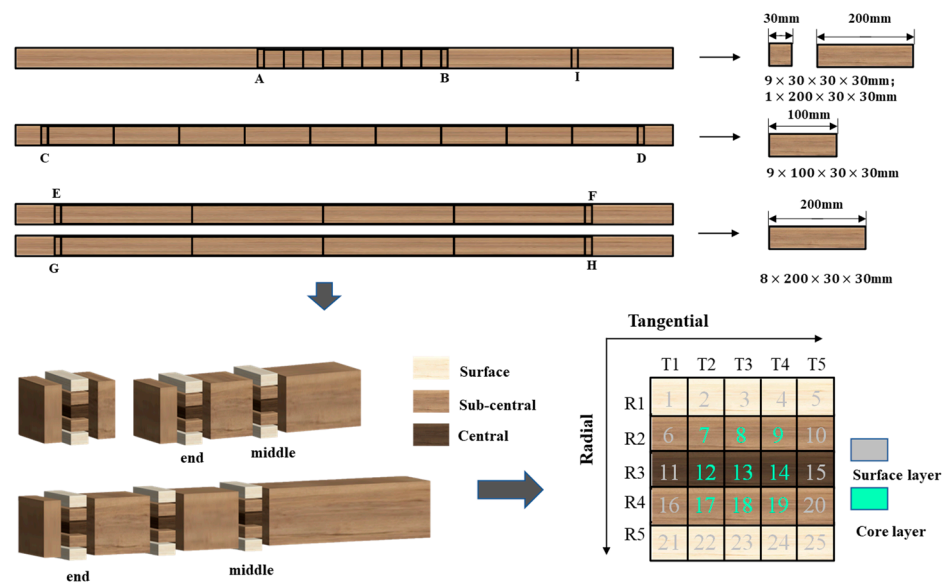
Figure 1. Schematic of samples preparation. Slices marked with A, B and I; C and D, E and F, G and H were used for the determination of the MC of the lumber.

2.3. Test Method

2.3.1. Wood Drying

Prior to drying, each sample was marked in the middle location along the tangential and radial direction, and then the dimensions were measured using a digital vernier caliper in the marked line and the mass of the samples using a balance. Thereafter, they were dried in a constant temperature and humidity chamber according to the parameters (Figure 2). To obtain an obvious collapse for the comparison, the drying condition in this study is slightly severe. The relative humidity was maintained at 65% in the whole drying process, while the temperature increased from room temperature to 70 °C (68 h later), and then maintained constant until end of drying. The samples were periodically taken out from the chamber to measure their dimensions and weight; as a result, the MC and shrinkage at this moment can be calculated according to the obtained data. When the MC of samples decreased to approximately 50, 30, and 12%, three samples were taken out from each group for MC distribution and difference measurement.
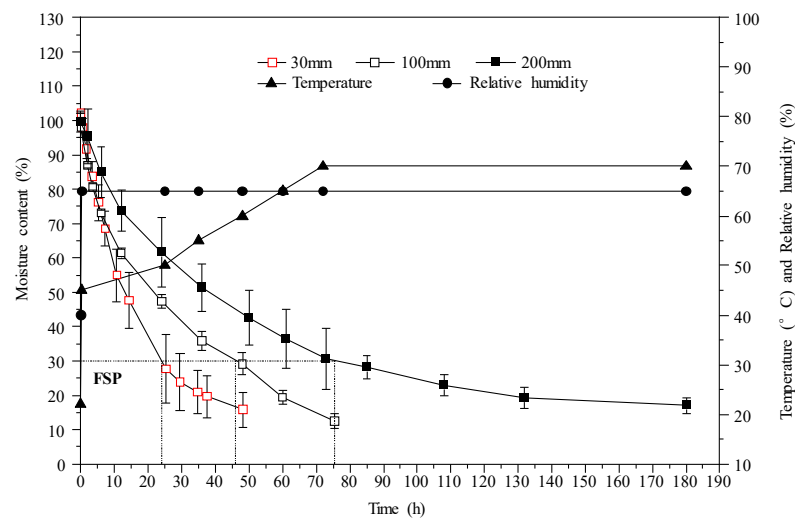
Figure 2. Drying curves of the samples and the temperature and humidity in the chamber against drying time.

2.3.2. Moisture Content Determination

The moisture content of samples was calculated using Equation (1) according to the National Standard of GB/T1931-2009:

$$MC = 100 \times (Mi - Mo)/Mo \qquad (1)$$

where *Mi* is the initial mass of samples (g) and *Mo* is the mass of oven-dried samples (g).

2.3.3. Moisture Content Distribution and Difference

Three samples were taken out from each group as their MC decreased to approximately 50%. After measuring the mass and dimensions, thin slices were sawn from the samples for measuring the MC distribution and difference (Figure 1). For 30 mm samples, one 10 mm slice was sawn in middle locations; for 100 mm samples, two 10 mm slices were sawn in the middle and end locations, respectively; for 200 mm samples, three 10 mm slices were sawn in the middle, one quarter, and end locations, respectively. After that, a slice was marked and numbered as shown in Figure 1; then, it was dissected into 25 small blocks. The MC of each block was calculated using equation 1 based on the oven-dry method. Consequently, the MC distribution and difference in the tangent and radial directions can be obtained by the MC of each block. For example, T1 demonstrates the first tangential layer, the MC of which is the average MC of the blocks numbered as 1, 6, 11, 16, and 21. The same measurements were also conducted when MC of the samples reached approximately 30% and 12%.

2.3.4. Shrinkage

The tangential and radial dimensions of samples were measured during drying, and they were used for transversal area calculation. The transversal shrinkage (*S*) of samples was calculated using Equation (2):

$$S = 100 \times (Ai - Af)/Ai \qquad (2)$$

where *Ai* (mm^2) and *Af* (mm^2) are the initial and final transversal areas of the samples corresponding to *MCi* and *MCf*, respectively.

2.3.5. Statistical Analysis

A multiple comparison was first applied to an analysis of variance (ANOVA) using SPSS to assess the effect of sample length on water transfer and shrinkage of wood, and significant differences between mean values of samples were determined using Duncan's multiple range tests ($p < 0.05$).

3. Results and Discussion

3.1. Drying Rate

The curves of moisture content, drying temperature, and humidity during the drying process are presented in Figure 2. The relevant data of initial and final MC, drying time, and drying rate above and below the FSP are summarized in Table 1. The moisture of *Eucalyptus urophylla* wood decreased fast when their MC was above the FSP (approximately 30%), especially for the shortest samples (30 mm); however, moisture content decreased slowly as the average MC of wood approached the FSP, and in particular, the decrease of 200 mm samples became more and more slow with the decrease of the average MC (Figure 2). A similar result was also obtained by a previous study [39]. It can also be clearly seen that the average drying rates of all samples above the FSP were significantly higher than that below the FSP (Table 2). The drying rate was significantly affected by sample length when the MC was above the FSP and presented an exponential decrease with the increase of sample length (Figure 3). However, below the FSP, the drying rate of the 30 and 100 mm samples were almost the same, and there was no noticeable relationship between drying rate and sample length. Free water is removed mostly by the capillary force from wood internal to the surfaces; however, bound water in wood is discharged by diffusion. The

different dewatering mechanism results in fast and slow water removal above and below the FSP, respectively [29,39,40]. Below the FSP, sample size significantly resists bound water diffusion, leading to a much lower drying rate.

Table 1. Initial and final moisture content (MC), drying time, and drying rate of all samples.

Sample Length (mm)	Initial MC (%)	Final MC (%)	Drying Time (h)			Drying Rate (%.h^{-1})		
			>FSP	<FSP	Total	>FSP	<FSP	Total
30	102.1	15.8	25	23	48	2.85	0.62	1.80
100	98.1	12.5	48	28	76	1.42	0.63	1.13
200	99.7	17.1	73	107	180	0.95	0.12	0.46

Table 2. Moisture content difference between middle and surface layers along tangential and radial direction when the average MC of the samples was at 50, 30, and 12%.

SL (mm)	100						200					
Location	Middle			End			Middle			End		
Average MC (%)	50	30	12	50	30	12	50	30	12	50	30	12
Tangential	28.9Aa	16.6Bb	9.8Dd	18.6Gg	4.0Hh	1.9Ii	31.4Aa	32.1Bc	1.2Ef	21.7Gg	4.9Hh	0.0Ii
Radial	27.8Aa	17.6Bb	10.4Dd	15.5Gg	4.3Hh	2.1Ii	21.8Aa	30.6Bc	1.6Ef	14.9Gg	5.6Hh	0.8Ii

SL: sample length. Means followed by the same capital letter do not differ significantly between the tangential and radial directions ($p < 0.05$) according to Duncan's multiple range tests at the same average MC. Means followed by the same lowercase letter do not differ significantly in same direction between 100 and 200 mm at the same average MC ($p < 0.05$) according to Duncan's multiple range tests.


$$Y = -1.022 \ln(x) + 6.2735$$

$$R^2 = 0.9833$$
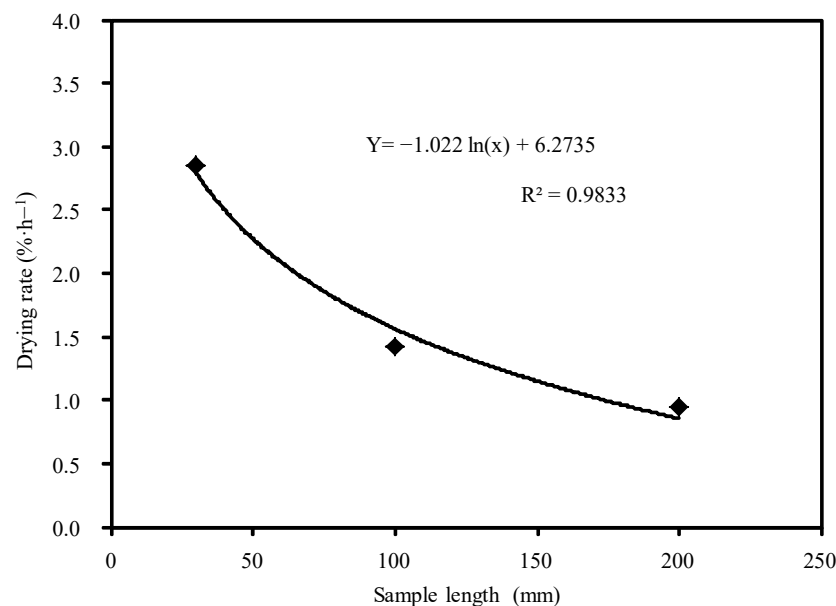
Figure 3. Drying rate against sample length above FSP.

3.2. Wood Moisture Distribution and MC Difference

3.2.1. Moisture Distribution and Difference along Tangential and Radial Directions

The MC distributions in the middle and end location of the 100 and 200 mm samples along the tangential and radial directions are shown in Figure 4a–d. The MC distributions presented a similar tendency in the middle and end locations along the tangential and radial directions, namely, the MC was more non-uniform when wood has a high MC and became even as MC decreased. Figure 4 demonstrates that the MC in the central layer was the highest, followed by the sub-central layers and then the surface layers.
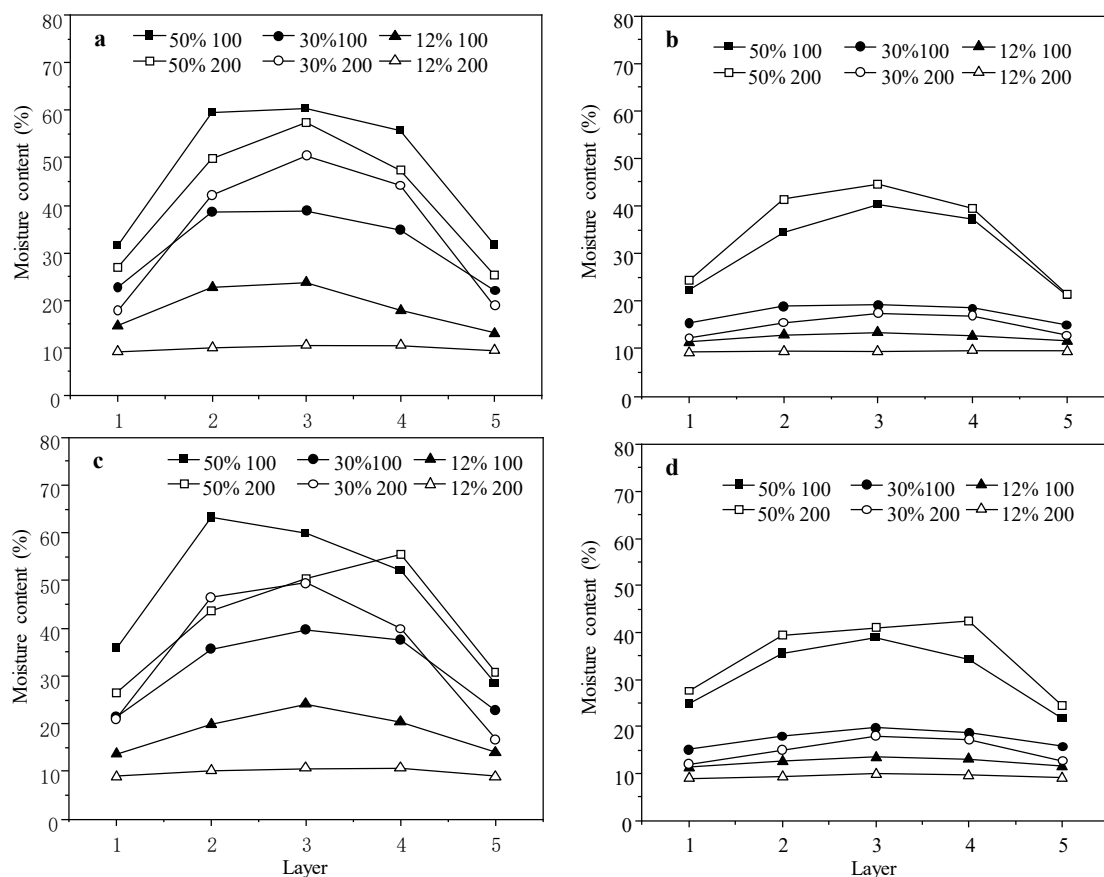
Figure 4. Moisture content distribution along the tangential direction: (**a**) middle location; (**b**) end location and radial direction; (**c**) middle location; (**d**) end location. Closed and open symbols refer to 100 and 200 mm samples, respectively.

The MC difference between the surface layers and sub-central layers along both tangential and radial directions were greater than that between the sub-central layers and central layer. In the middle location, the MC differences along the tangential and radial directions were obvious when the average MC was 50 and 30%, but in the end location, the MC difference were apparent only at an average MC of 50%.

Table 2 summarizes the MC differences between the central and surface layers along the tangential and radial directions in the middle and end locations at three average MC stages. In the end locations, there were no significant differences of MC difference between the tangential and radial directions for the same length or different length samples at all MC stages ($p < 0.05$). This can also be observed in the middle location for all samples when the average MC was at 50%.

However, there were significant differences of MC difference along the tangential and radial directions in the middle locations between the 100 and 200 mm samples when the average MC was at 30 and 12% ($p < 0.05$). These indicate that the MC distributions and MC difference along the tangential and radial directions in the middle location of samples are significantly affected by sample length when their average MC are close to or lower than the FSP. The ANOVA results also indicated that the locations in wood have a significant influence on MC distribution, but the effect of dimension depends on the final MC of the wood. This is probably due to the unique microstructure and chemical composition of the fast-growing *Eucalyptus urophylla* × *E. grandis* trees.

3.2.2. Moisture Content Distribution and MC Difference along Longitudinal Direction

Figure 5 illustrates the MC distribution and MC difference of the 100 and 200 mm samples along the wood longitudinal direction. The MC in the end locations was lower than that in the sub-middle and middle locations not only in the central (Figure 5b) and the sub-central (Figure 5c) layers, but also in the surface layers (Figure 5d). For the 200 mm sample, the MC in the middle and sub-middle locations were almost the same when the average MC was at 50 and 12%, but the MC in the sub-middle location was obviously smaller than that in the middle when the average MC was at 30%, presenting an apparent decreasing whereby the highest was in the middle, followed by the sub-middle, and the lowest was in the end. This trend was obvious in the central layer (Figure 5b), sub-central layer (Figure 5c), and surface layer (Figure 5d).
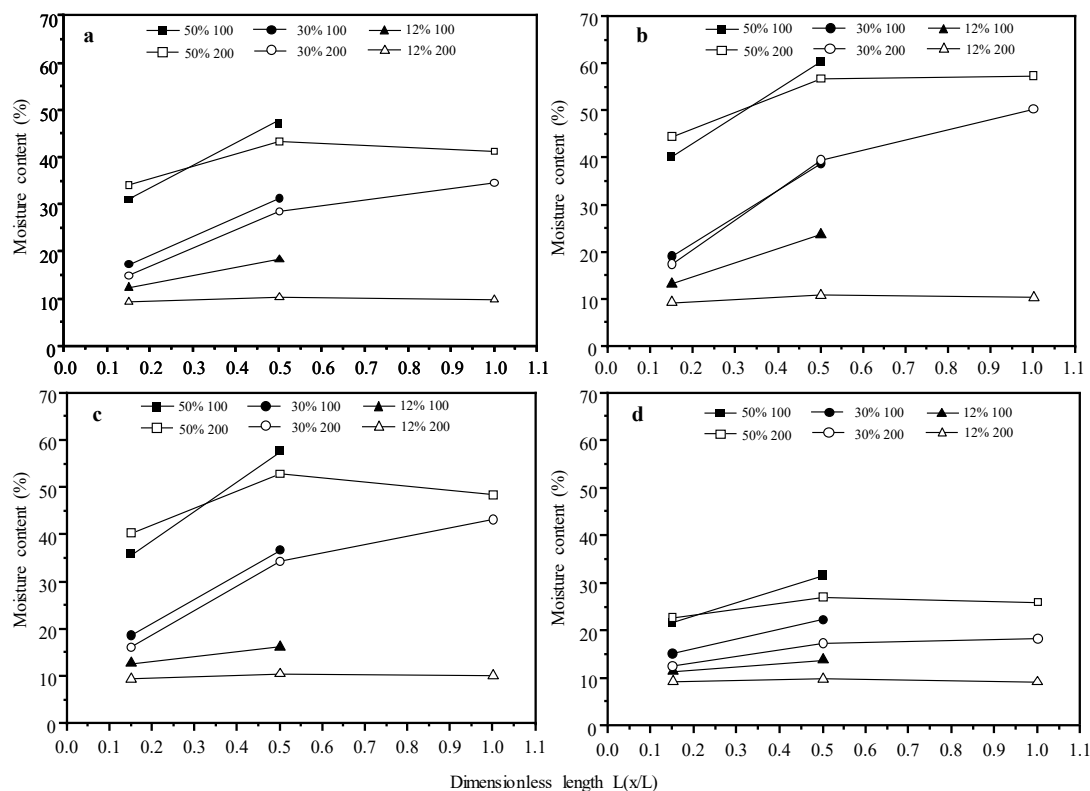
Figure 5. Moisture content distribution along the longitudinal direction: (**a**) average of the central, sub-central and surface, (**b**) central, (**c**) sub-central, (**d**) surface. The horizontal axis (dimensionless length) indicates the relative distance of the end, sub-middle, and middle locations to the half of 200 mm samples. Closed and open symbols refer to 100 and 200 mm samples, respectively.

Table 3 shows the MC difference between the middle and end location of the 100 mm samples and sub-middle and end location of the 200 mm samples along the longitudinal direction at three average MC stages. When the average MC was at 50 and 30%, for the same length samples, there were no significant differences in MC difference between the central and sub-central layers, but a significant MC difference was observed in the surface layer ($p < 0.05$). When the average MC was at 12%, for the 100 mm samples, a significant MC difference was observed in the central layer compared with the sub-central and surface layers, but for the 200 mm samples, the MC difference in the surface layer showed significant differences compared with the central and sub-central layers ($p < 0.05$). For different length samples, when the average MC was at 50 and 12%, there were significant differences in MC difference in the central, sub-central, and surface layers ($p < 0.05$), but when the average MC was at 30%, no significant differences in MC difference were observed in the central and sub-central layer, while the surface layer showed significant differences ($p < 0.05$). All

these indicate that MC distributions and MC difference along the longitudinal direction of wood are significantly affected by sample length when the wood has a higher or lower MC.

Table 3. Moisture difference along the longitudinal direction in central, middle, and surface layers when average MC of the samples was at 50, 30, and 12%.

Sample Length (mm)	100			200		
Dimensionless Length	0.5–0.15			0.5–0.15		
MC (%)	50	30	12	50	30	12
Central layer	20.2Aa	19.8Aa	10.3Aa	12.3Ab	22.1Aa	1.5Ab
Sub-central layer	21.8Aa	18.1Aa	3.5Ba	12.5Ab	18.2Aa	1.1Ab
Surface layer	9.9Ba	7.2Ba	2.4Ba	4.3Bb	4.8Bb	0.6Bb

Means followed by the same capital letter do not differ significantly between central, middle, and surface layers at the same MC ($p < 0.05$) according to Duncan's multiple range tests. Means followed by the same lowercase letter do not differ significantly in same location between 100 and 200 mm at the same MC ($p < 0.05$) according to Duncan's multiple range tests.

3.3. Moisture Transfer

Figure 6 shows the relationship between the drying rate and the ratio of end areas to the total surface areas of three sets of samples. The drying rate significantly increased linearly with the ratio of end areas to total area of samples when the MC was above the FSP (Figure 6a, $R^2 = 0.9997$). When the MC was above the FSP, although the side areas of the 200 and 100 mm samples are 6.7 and 3.3 times that of the 30 mm samples, their drying rates are 33% and 50% of the 30 mm samples, respectively. These results are in agreement with a previous report [40], which indicates that free water is removed mostly from both ends of wood along the fiber direction. The 30 mm samples have a shorter transfer distance in the fiber direction, leading to a much faster removal of free water.
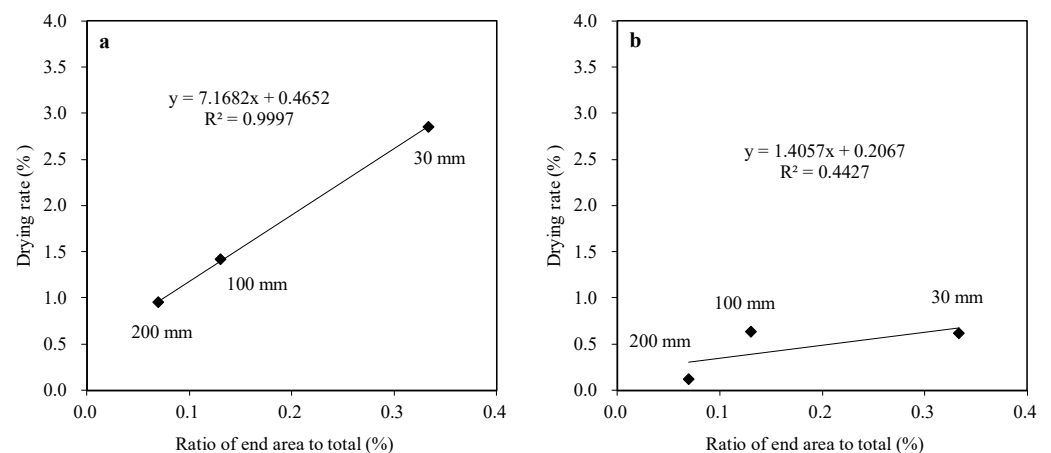
Figure 6. Drying rate against ratio of side areas to total of samples (**a**) above the FSP, (**b**) below the FSP.

However, there were no apparent linear relationships between the drying rate and the ratio of end areas to the total area of samples when the MC was below the FSP (Figure 6b, $R^2 = 0.4427$). The drying rates were almost the same for the 30 and 100 mm samples with significantly different side areas, indicating that most bound water diffuses also from the end of the wood along the longitudinal direction. However, for the 200 mm samples, due to the longest transfer distance from the wood central to the ends, their drying rates were much lower than that of the 30 and 100 mm samples. This further demonstrates that bound water in the 200 mm samples also diffuses mostly from the wood central to both ends along the longitudinal direction, coinciding with previous results [36]. Additionally, it can be seen that sample length has a significant influence on bound water migration as it is longer than 200 mm in this study.

3.4. Wood Shrinkage and Collapse

The transversal shrinkage curves of the samples during the drying are shown in Figure 7. Generally, normal shrinkage occurs at an MC below the FSP [41]. However, all samples shrink both in the tangential and radial direction above the FSP. A previous study also observed a similar phenomenon of shrinkage [42]. This shrinkage above the FSP, known as collapses, are caused by capillary tension resulting from free water migration in the wood cell lumen [43]. As the MC of the samples decreased to the FSP, wood shrinkage became more apparent and increased significantly with MC decrease. The shrinkage in this stage is termed as normal shrinkage and is linearly increased with decreasing of the MC of wood. From Figure 7, it can be seen that three sets of samples all collapsed from the beginning of drying and increased slightly with MC decrease. The transversal collapses of the 30 and 100 mm samples were almost same; however, those of the 200 mm samples are slightly greater. The ANOVA results indicated that sample length has a significant influence on both tangential and radial shrinkage, suggesting that sample length affects wood collapse. Although moisture transfer is mainly in the longitudinal direction for all three sample lengths, and the moisture content decreases exponentially with an increase in sample length, the collapse of the samples with these three lengths was not so noticeable. These findings indicate that the drying rate of free water has less effect on collapse for samples with a length below 200 mm. When the MC is lower than the FSP, the collapse of the 30 and 100 mm samples had a small change, but the collapse of the 200 mm samples increased to a peak after the MC reached the FSP and subsequently deceased with MC reducing due to the recovery of cell walls [41]. The differences of final shrinkage of three sets of samples were not great in this study. These results indicate that the collapse recovery of wood is also significantly affected by sample length.
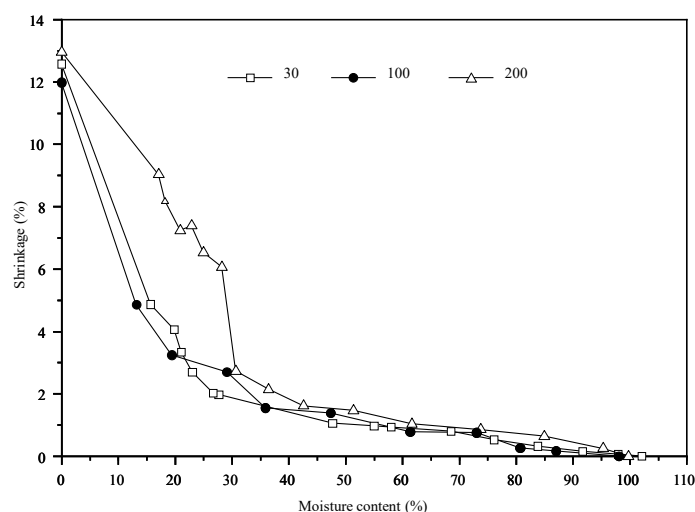

Figure 7. Transversal shrinkage versus MC of 30, 100, and 200 mm samples during drying.

4. Conclusions

The transfer and distribution of water in *Eucalyptus urophylla* wood along the tangential, radial, and longitudinal directions during conventional kiln drying were investigated using samples with three lengths. Meanwhile, the deformation of different samples was observed during drying. The results revealed that the drying rate decreased exponentially with sample lengths above the fiber saturated point (FSP), while no apparent relationship between drying rate and sample length was observed below the FSP; moisture distribution along wood in the three directions were more non-uniform above the FSP than that below the FSP, which was more apparent inside the samples; and the greatest moisture content (MC) gradient occurred between the surface and sub-central layers along the tangential and radial directions, which was between the end and sub-middle locations along the longitudinal direction. Although samples are less than 200 mm, the effect of sample length

on the moisture distribution and MC difference were dependent on the locations and moisture stage of wood; most of the free water and bound water transferred from the wood central to the ends along the longitudinal directions for all samples. Bound water flow was significantly small as the wood length exceeded 200 mm. Furthermore, sample length affects wood collapse and its recovery, but the drying rate has a lesser effect on collapse for samples with a length below 200 mm. The obtained outcomes will provide scientific support to prepare effective drying schedules and investigate the underlying mechanism of wood collapse during water removal.

Author Contributions: Writing—original draft preparation, M.K., T.Z. and X.S.; writing—review and editing, H.L. All authors have read and agreed to the published version of the manuscript.

Data Availability Statement: Not applicable.

References

1. De Aguiar Ferreira, J.; Stape, J. Productivity gains by fertilisation in *Eucalyptus urophylla* clonal plantations across gradients in site and stand conditions. *South. For.* **2009**, *71*, 253–258. [CrossRef]
2. Carignato, A.; Moraes, C.B.D.; Zimback, L.; Mori, E.S. Genetic Resistance to Rust of *Eucalyptus urophylla* Progenies. *Floresta Ambiente* **2018**, *25*. [CrossRef]
3. Stape, J.L.; Binkley, D.; Ryan, M.G.; Fonseca, S.; Loos, R.A.; Takahashi, E.N.; Silva, C.R.; Silva, S.R.; Hakamada, R.E.; Ferreira, J.M.d.A. The Brazil Eucalyptus Potential Productivity Project: Influence of water, nutrients and stand uniformity on wood production. *For. Ecol. Manag.* **2010**, *259*, 1684–1694. [CrossRef]
4. Anzum, R. Factors that affect LoRa Propagation in Foliage Medium. *Procedia Comput. Sci.* **2021**, *194*, 149–155. [CrossRef]
5. Yang, L. Effect of temperature and pressure of supercritical CO_2 on dewatering, shrinkage and stresses of Eucalyptus Wood. *Appl. Sci.* **2021**, *11*, 8730. [CrossRef]
6. França, F.J.N.; Maciel, A.P.V.-B.; França, T.S.F.A.; da Silva, J.G.M.; Batista, D.C. Air-drying of seven clones of *Eucalyptus grandis* × *Eucalyptus urophylla* wood. *BioResources* **2019**, *14*, 6591–6607. [CrossRef]
7. Lei, W.; Zhang, Y.; Ge, L.; Yu, W. Study on suitability manufacture process of structure *Eucalyptus scrimber*. *J. For. Eng.* **2022**, *7*, 46–52.
8. Nutto, L.; Malinovski, R.A.; Brunsmeier, M.; Schumacher Sant'Anna, F. Ergonomic aspects and productivity of different pruning tools for a first pruning lift of *Eucalyptus grandis* Hill ex Maiden. *Silva Fenn.* **2013**, *47*, 1026. [CrossRef]
9. Yang, L.; Jin, H. Effect of heat treatment on the physic-mechanical characteristics of *Eucalyptus urophylla* S.T. Blake. *Materials* **2021**, *14*, 6643. [CrossRef]
10. Chen, Y.; Zhu, J. Study on bending characteristics of fast growing eucalyptus bookcase shelves by using burgers model. *Wood Res.* **2019**, *64*, 137–144.
11. Yang, L.; Zheng, J.; Huang, N. The Characteristics of Moisture and Shrinkage of *Eucalyptus urophylla* × E. Grandis Wood during Conventional Drying. *Materials* **2022**, *15*, 3386. [CrossRef] [PubMed]
12. Paschalina, T.; Vasiliki, K. Chemical characterization of wood and bark biomass of the invasive species of tree-of-heaven (*Ailanthus altissima* (Mill.) Swingle), focusing on its chemical composition horizontal variability assessment. *Wood Mater. Sci. Eng.* **2022**, *17*, 469–477.
13. Tu, D.; Chen, C.; Zhou, Q.; Ou, R.; Wang, X. Research progress of thermo-mechanical compression techniques for wood products. *J. For. Eng.* **2021**, *6*, 13–20.
14. Fu, Z.; Zhou, Y.; Gao, X.; Liu, H.; Zhou, F. Changes of water related properties in radiata pine wood due to heat treatment. *Constr. Build. Mater.* **2019**, *227*, 116692. [CrossRef]
15. Ruwoldt, J.; Kai, T. Alternative wood treatment with blends of linseed oil, alcohols and pyrolysis oil. *J. Bioresour. Bioprod.* **2022**, *7*, 278–287. [CrossRef]
16. Li, J.; Ma, E. Influence of heat treatment and delignification on hygroscopicity limit and cell wall saturation of southern pine wood. *J. For. Eng.* **2021**, *6*, 61–68.
17. Feng, X.H.; Chen, J.Y.; Yu, S.X.; Wu, Z.H.; Huang, Q.T. Mild hydrothermal modification of beech wood (*Zelkova schneideriana* Hand-Mzt): Its physical, structural, and mechanical properties. *Eur. J. Wood Wood Prod.* **2022**, *80*, 933–945. [CrossRef]
18. Shen, Y.; Gao, Z.; Hou, X.; Chen, Z.; Jiang, J.; Sun, J. Spectral and thermal analysis of *Eucalyptus* wood drying at different temperature and methods. *Dry. Technol.* **2019**, *38*, 313–320. [CrossRef]
19. Lahr, F.A.; Nogueira, M.C.; Araujo, V.A.D.; Vasconcelos, J.S.; Christoforo, A.L. Physical-mechanical characterization of *Eucalyptus urophylla* wood. *Eng. Agríc.* **2017**, *37*, 900–906. [CrossRef]

20. Salas, C.; Moya, R. Kiln-, solar-, and air-drying behavior of lumber of *Tectona grandis* and *Gmelina arborea* from fast-grown plantations: Moisture content, wood color, and drying defects. *Dry. Technol.* **2014**, *32*, 301–310. [CrossRef]
21. Zongying, F.; Zhao, J.; Lv, Y.; Huan, S.; Cai, Y. Stress characteristics and stress reversal mechanism of white birch (*Betula platyphylla*) disks under different drying conditions. *Maderas Cienc. Tecnol.* **2016**, *18*, 361–372. [CrossRef]
22. Meng, Y.; Chen, G.; Hong, G.; Wang, M.; Gao, J.; Chen, Y. Energy efficiency performance enhancement of industrial conventional wood drying kiln by adding forced ventilation and waste heat recovery system: A comparative study. *Maderas Cienc. Tecnol.* **2019**, *21*, 545–558. [CrossRef]
23. Sepulveda-Villarroel, V.; Perez-Peña, N.; Salinas-Lira, C.; Salvo-Sepulveda, L.; Elustondo, D.; Ananias, R.A. The development of moisture and strain profiles during predrying of *Eucalyptus nitens*. *Dry. Technol.* **2016**, *34*, 428–436. [CrossRef]
24. Kong, L.; Zhao, Z.; He, Z.; Yi, S. Development of schedule to steaming prior to drying and its effects on *Eucalyptus grandis* × *E. urophylla* wood. *Eur. J. Wood Wood Prod.* **2018**, *76*, 591–600. [CrossRef]
25. Peres, M.L.; Delucis, R.d.A.; Gatto, D.A.; Beltrame, R. Solid wood bending of *Eucalyptus grandis* wood plasticized by steam and boiling. *Ambiente Construído* **2015**, *15*, 169–177. [CrossRef]
26. Zhang, Y.; Miao, P.; Zhuang, S.; Wang, X.; Xia, J.; Wu, L. Improving the dry-ability of *Eucalyptus* by pre-microwave or pre-freezing treatment. *J. Nanjing For. Univ. (Nat. Sci. Ed.)* **2011**, *35*, 61–64.
27. Chafe, S.C. *Collapse: An Introduction*; CSIRO Division of Forest Products: Canberra, Australia, 1992.
28. Skaar, C. *Wood-Water Relations*; Springer Science & Business Media: New York, NY, USA, 2012.
29. Siau, J.F. *Transport Processes in Wood*; Springer Science & Business Media: New York, NY, USA, 2012.
30. Amer, M.; Kabouchi, B.; El Alami, S.; Azize, B.; Rahouti, M.; Famiri, A.; Fidah, A. Water sorption/desorption kinetics and convective drying of *Eucalyptus globulus* wood. *J. Korean Wood Sci. Technol.* **2019**, *47*, 557–566. [CrossRef]
31. Ahmed, S.A.; Chun, S.K. Permeability of *Tectona grandis* L. as affected by wood structure. *Wood Sci. Technol.* **2011**, *45*, 487–500. [CrossRef]
32. Monteiro, T.C.; Lima, J.T.; Silva, J.R.M.d.; Rezende, R.N.; Klitzke, R.J. Water flow in different directions in *Corymbia citriodora* wood. *Maderas Cienc. Tecnol.* **2020**, *22*, 385–394. [CrossRef]
33. Engelund, E.T.; Thygesen, L.G.; Svensson, S.; Hill, C.A. A critical discussion of the physics of wood-water interactions. *Wood Sci. Technol.* **2013**, *47*, 141–161. [CrossRef]
34. Monteiro, T.C.; Lima, J.T.; Abreu Neto, R.; Ferreira, C.A. Importance of pits in *Corymbia citriodora* (Hook.) KD Hill & LAS Johnson (Myrtaceae) wood permeability. *Floresta Ambiente* **2020**, *28*, e20200012. [CrossRef]
35. Baraúna, E.E.P.; Lima, J.T.; Vieira, R.d.S.; Silva, J.R.M.d.; Monteiro, T.C. Effect of anatomical and chemical structure in the permeability of Amapá wood. *Cerne* **2014**, *20*, 529–534. [CrossRef]
36. Gao, Y.; Li, Y.; Ren, R.; Chen, Y.; Gao, J. Effect of weak acid modification on the structure and properties of heat-treated Chinese fir. *J. For. Eng.* **2021**, *6*, 49–55.
37. Pelit, H.; Emiroglu, F. Effect of water repellents on hygroscopicity and dimensional stability of densified fir and aspen woods. *Drv. Ind.* **2020**, *71*, 29–40. [CrossRef]
38. Sedlar, T.; Šefc, B.; Drvodelić, D.; Jambreković, B.; Kučinić, M.; Ištok, I. Physical properties of juvenile wood of two paulownia hybrids. *Drv. Ind.* **2020**, *71*, 179–184. [CrossRef]
39. Monteiro, T.C.; Lima, J.T.; Hein, P.R.G.; da Silva, J.R.M.; Neto, R.d.A.; Rossi, L. Drying kinetics in *Eucalyptus urophylla* wood: Analysis of anisotropy and region of the stem. *Dry. Technol.* **2022**, *40*, 2046–2057. [CrossRef]
40. He, Z.; Ye, M.; Zhang, Y.; Wu, F.; Fu, M.; Sun, F.; Liu, X. Effect of seed size and drying temperature on the hot air drying kinetics and quality of Chinese hickory (*Carya cathayensis*) storage. *J. Food Process. Preserv.* **2021**, *45*, 15488. [CrossRef]
41. Li, Z.; Jiang, J.; Lyu, J.; Cao, J. Orthotropic Viscoelastic Properties of Chinese Fir Wood Saturated with Water in Frozen and Non-frozen States. *For. Prod. J.* **2021**, *71*, 77–83. [CrossRef]
42. Yang, L.; Liu, H. Study of the collapse and recovery of *Eucalyptus urophydis* during conventional kiln drying. *Eur. J. Wood Wood Prod.* **2021**, *79*, 129–137. [CrossRef]
43. Gonya, N.; Naghizadeh, Z.; Wessels, C. An investigation into collapse and shrinkage behaviour of *Eucalyptus grandis* and *Eucalyptus grandis*-urophylla wood. *Eur. J. Wood Wood Prod.* **2022**, *80*, 139–157. [CrossRef]